U.S. DEPARTMENT OF ENERGY | Office of Science

NSTX-U

Modelling of VDEs with M3D-C1

D.Pfefferlé[1]

S.Jardin[1] **N.Ferraro**[1] **C.Myers**[1] **A.Bhattacharjee**[1]

[1] *PPPL, Princeton 08540 NJ, USA*

APS-DPP 2016
San Jose, CA
November 1, 2016

PPPL

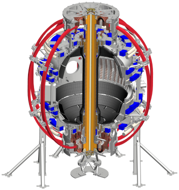

VDEs are inherent to diverted tokamak plasmas

external potential from PF coils

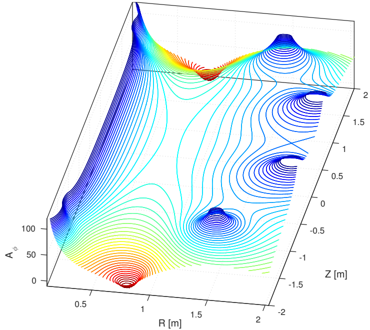

effective potential along Z

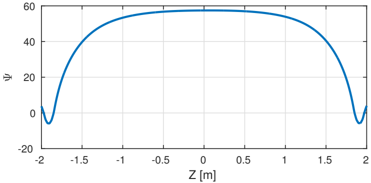

- diverted plasma on a saddle due to external field (PF coils) $\Rightarrow$ elongation, vertically unstable equilibrium
- conducting structures do not allow fast flux changes $\Rightarrow$ passive stabilisation + feedback control
- loss of vertical control leads to deleterious contact with wall
  - transfer/induction of current from core $\rightarrow$ halo $\rightarrow$ wall $\Rightarrow$ forces and stresses
  - scraping-off of $q_{edge} < 2 \Rightarrow$ 3D instabilities (kink), toroidal peaking of forces
  - thermal collapse, impurities $\Rightarrow$ breaking of flux surfaces, runaway electrons

Damaging power of VDEs calls for realistic modelling

- forces during VDEs lead to structural damages of PFCs, can result in machine shutdown
  - worst case VDE is a design drive for ITER
  - need for avoidance (preemptive measures) and mitigation (damage control)
- abundant experimental data to be analysed and interpreted
  - provide theoretical/modelling support
  - help interpret measurements and optimise diagnostics for wall/halo currents

Basic/fundamental questions:

1. What are the key dynamics/regimes/phases of VDEs ?
   - rich literature, reduced models, linear theories, Halo/Hiro debate
   - self-consistently assembling the pieces of the puzzle is not trivial (stiffness)
2. Can we simulate/model VDEs accurately enough to feel confident about predictions for ITER ?
   - **difficult**: 2D + prescriptions OK, 3D not (yet) with realistic parameters
   - 3D: computationally far more expensive, profoundly richer physics than 2D

Phenomenology of VDEs serves as modelling targets

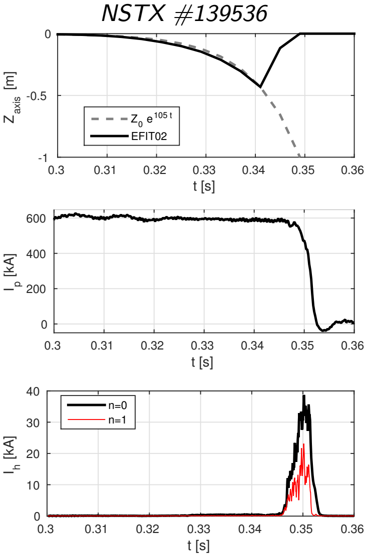

- drift phase [Pfefferlé, 2016]
  $t_D \sim (L_w/R_w)(I_p/I_d)(Z_d/Z_w)^2 \sim 30\text{ms}$
  - **slow** relaxation process
  - plasma mostly in force balance
  - advection ($\approx$ rigid body), inductive coupling with wall $\Rightarrow$ **implicit scheme**
- current quench $t_{CQ} \gtrsim L_p^*/R_p^* \sim 3ms$ [Wesley, 2006]
  - current transfer/induction from plasma to wall
  - flux scrape-off (advection-diffusion) + time-evolving resistivity via temperature
- normal wall currents $\Delta t_H \sim t_{CQ}$ [Myers, 2016]
  - shared/induced currents in resistive halo
  - early $n=1 \sim n=0$ components
  - counter-I_p rotation $\Omega R \sim 3\text{km/s} = 0.1 c_s$ for max 4 turns

M3D-C1 is a state-of-art FEM implicit code, suitable for modelling VDEs

Typical setup, parameters and recipe:

0.a 3 region **anisotropic mesh** for plasma, wall and vacuum

0.b Grad-Shafranov equilibrium reconstruction from experimental profiles (`geqdsk`) and coil currents

1. 2D nonlinear **implicit** runs, tuned to match realistic timescales
   - Spitzer resistivity $\times$ 30 $\Rightarrow$ Lundquist $S \sim 10^8 - 10^9$
   - 2cm wall with resistivity $\eta_w = 1.9 \times 10^{-6} \Omega m$
   - thermal conductivity $\kappa_T = 10^{-6} \kappa_0$
   - halo region: $n_h = 10^{18} m^{-3}$, $p_h = 8$ Pa, $T_h = 25$eV
     - effective temperature for halo resistivity $T_h = 9$eV
2. linear analysis launched at different times during 2D drift phase
   - monitor $n > 0$ modes, compare instantaneous growth rates with $n = 0$
3. 3D nonlinear **implicit** runs started when plasma almost contacts wall
   - 48 toroidal planes
   - 4608 cores for 300'000 CPU hours
   - still **in progress** due to NERSC queues

M3D-C1 2D nonlinear simulation of NSTX #132859

with $\eta_W = 1.9 \times 10^{-6}\Omega m$, $T_h = 9$eV

toroidal current density

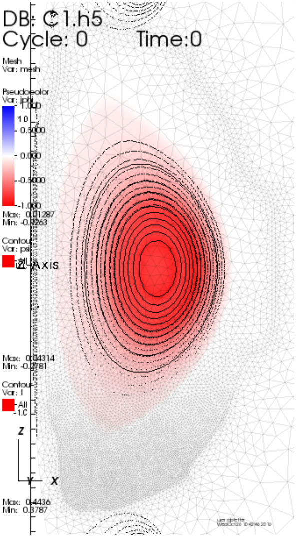

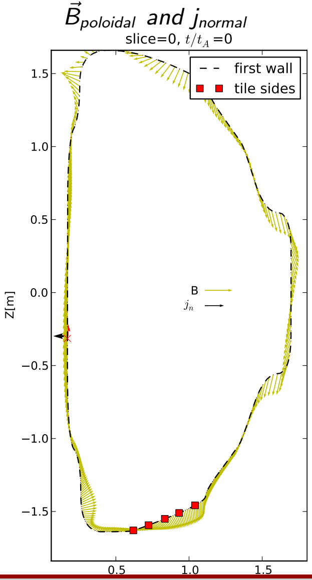

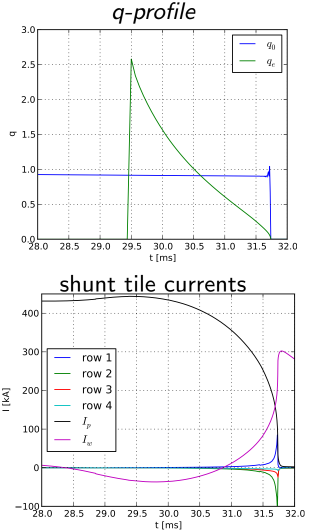

M3D-C1 2D nonlinear simulation of NSTX #132859

with $\eta_W = 1.9 \times 10^{-6}\Omega m$, $T_h = 9$eV

toroidal current density

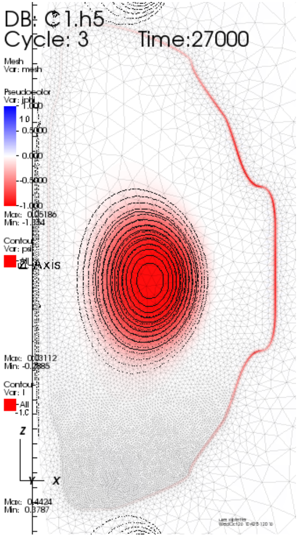

$\vec{B}_{poloidal}$ *and* j_{normal}

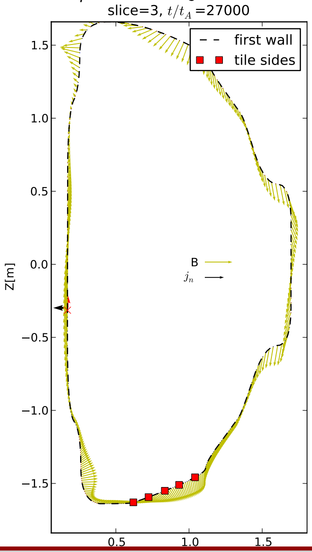

q-profile

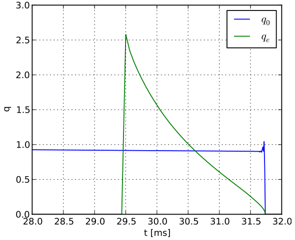

shunt tile currents

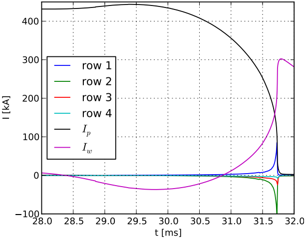

M3D-C1 2D nonlinear simulation of NSTX #132859

with $\eta_W = 1.9 \times 10^{-6}\Omega m$, $T_h = 9$eV

toroidal current density

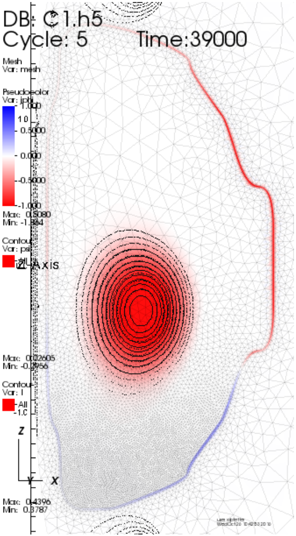

$\vec{B}_{poloidal}$ *and* j_{normal}

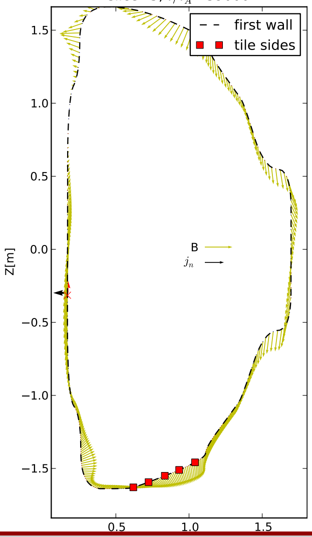

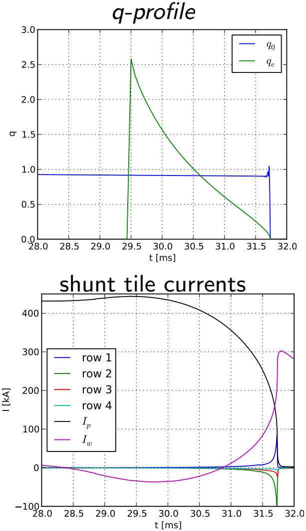

M3D-C1 2D nonlinear simulation of NSTX #132859

with $\eta_W = 1.9 \times 10^{-6}\Omega m$, $T_h = 9$eV

toroidal current density

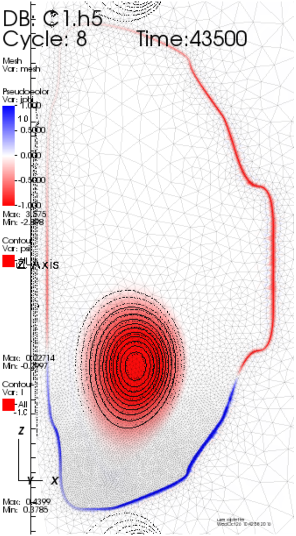

$\vec{B}_{poloidal}$ and j_{normal}

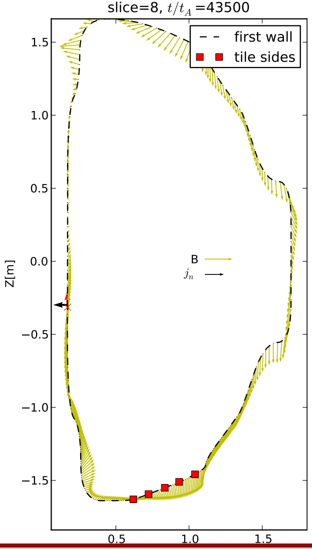

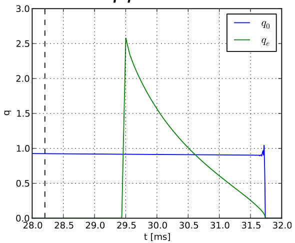

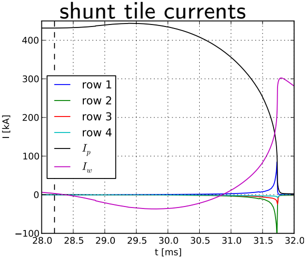

M3D-C1 2D nonlinear simulation of NSTX #132859

with $\eta_W = 1.9 \times 10^{-6}\Omega m$, $T_h = 9$eV

toroidal current density

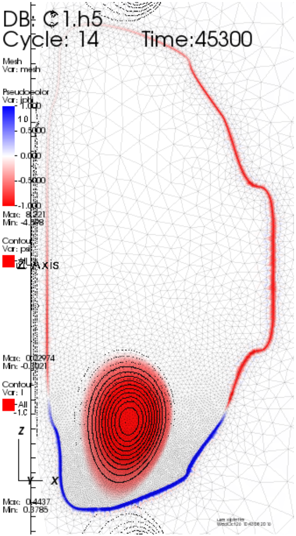

$\vec{B}_{poloidal}$ *and* j_{normal}

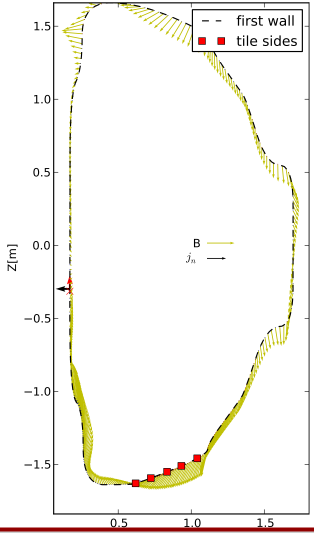

q-profile

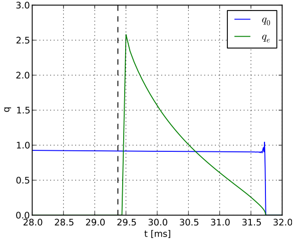

shunt tile currents

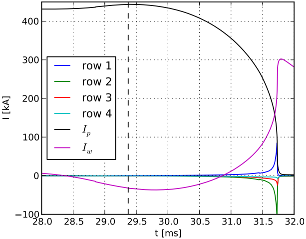

M3D-C1 2D nonlinear simulation of NSTX #132859

with $\eta_W = 1.9 \times 10^{-6}\Omega m$, $T_h = 9$eV

toroidal current density

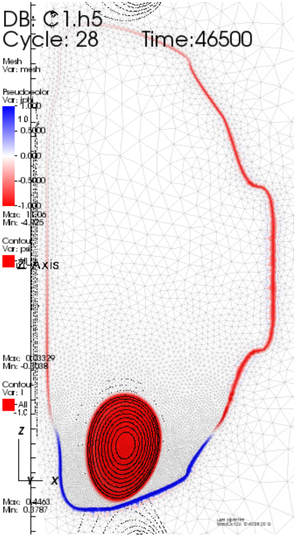

$\vec{B}_{poloidal}$ *and* j_{normal}

slice=28, t/t_A =46500

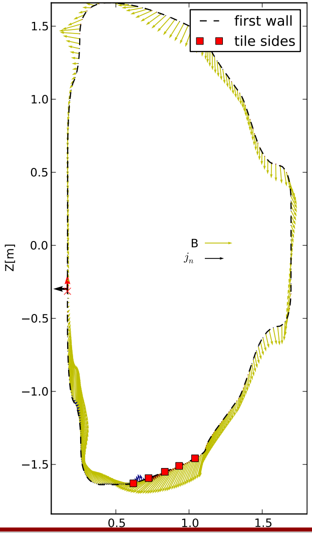

q-profile

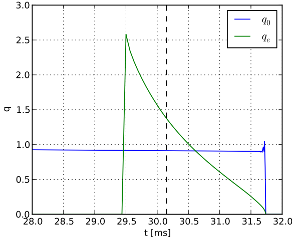

shunt tile currents

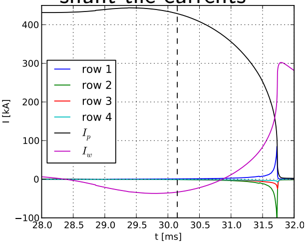

M3D-C1 2D nonlinear simulation of NSTX #132859

with $\eta_W = 1.9 \times 10^{-6}\Omega m$, $T_h = 9$**eV**

toroidal current density

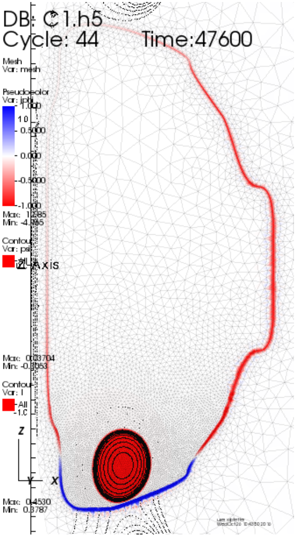

$\vec{B}_{poloidal}$ *and* j_{normal}

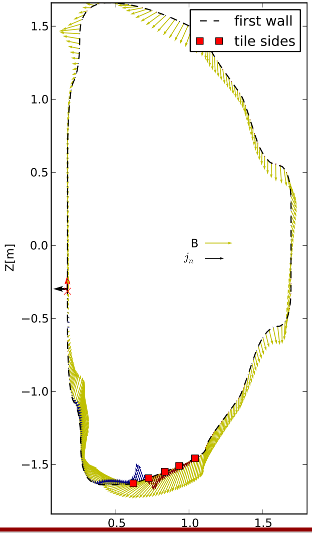

q-profile

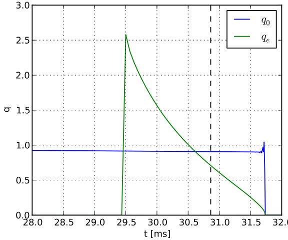

shunt tile currents

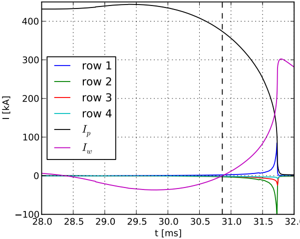

M3D-C1 2D nonlinear simulation of NSTX #132859

with $\eta_W = 1.9 \times 10^{-6}\Omega m$, $T_h = 9$eV

toroidal current density

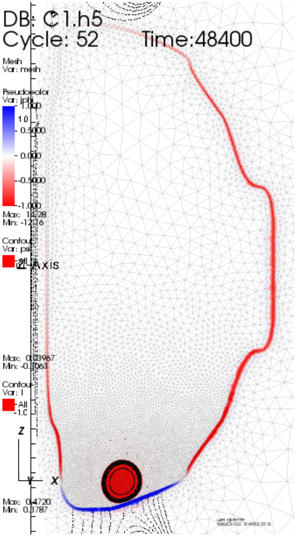

$\vec{B}_{poloidal}$ *and* j_{normal}

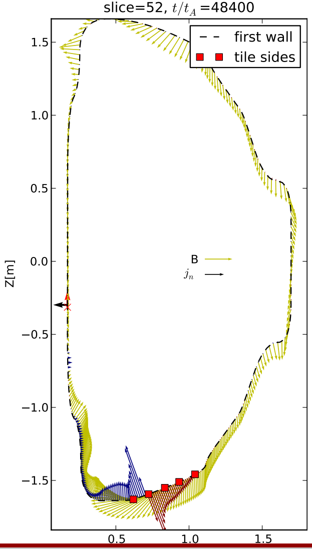

q-profile

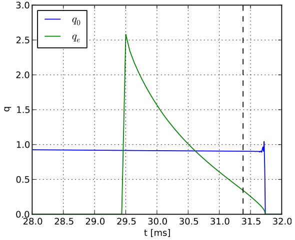

shunt tile currents

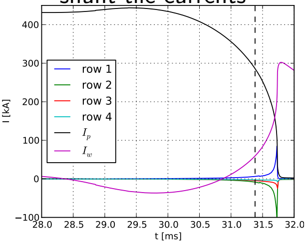

M3D-C1 2D nonlinear simulation of NSTX #132859

with $\eta_W = 1.9 \times 10^{-6} \Omega m$, $T_h = 9$**eV**

toroidal current density

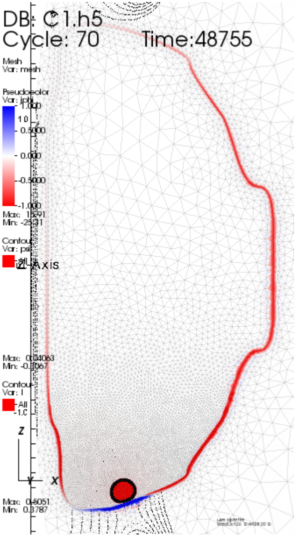

$\vec{B}_{poloidal}$ *and* j_{normal}

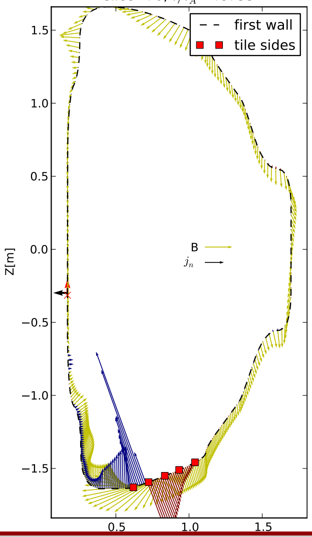

q-profile

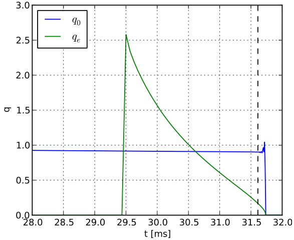

shunt tile currents

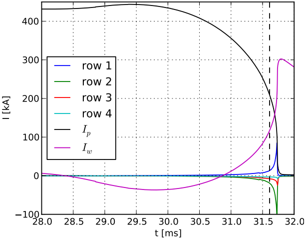

M3D-C1 2D nonlinear simulation of NSTX #132859

with $\eta_W = 1.9 \times 10^{-6}\Omega m$, $T_h = 9$eV

toroidal current density

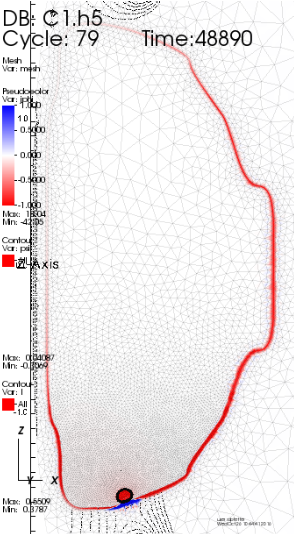

$\vec{B}_{poloidal}$ and j_{normal}

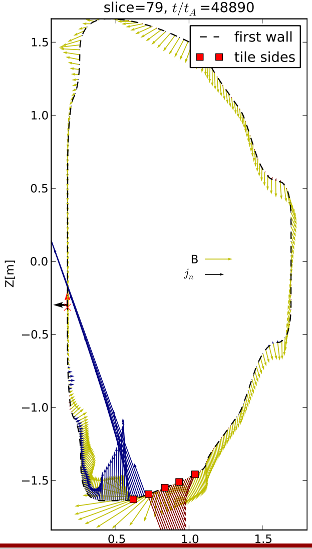

q-profile

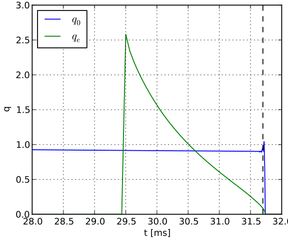

shunt tile currents

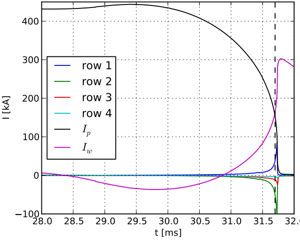

M3D-C1 2D nonlinear simulation of NSTX #132859

with $\eta_W = 1.9 \times 10^{-6} \Omega m$, $T_h = 9$eV

toroidal current density

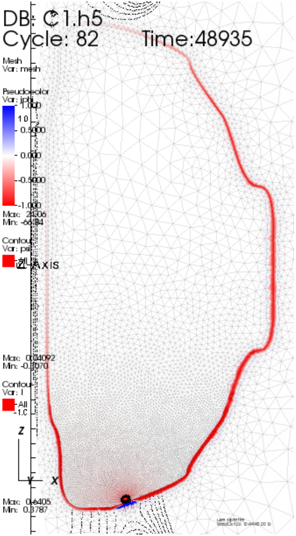

$\vec{B}_{poloidal}$ *and* j_{normal}

slice=82, t/t_A =48935

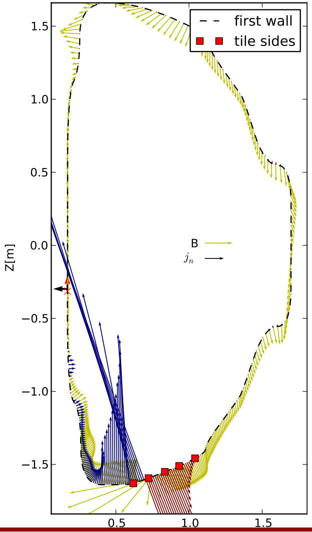

q-profile

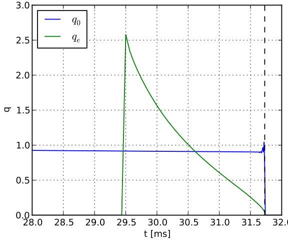

shunt tile currents

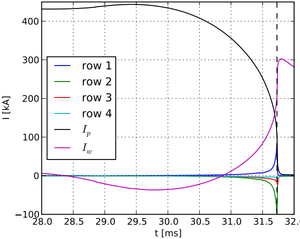

M3D-C1 2D nonlinear simulation of NSTX #132859

with $\eta_W = 1.9 \times 10^{-6}\Omega m$, $T_h = 9$eV

toroidal current density

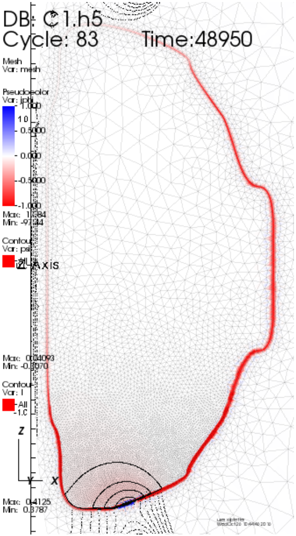

$\vec{B}_{poloidal}$ *and* j_{normal}

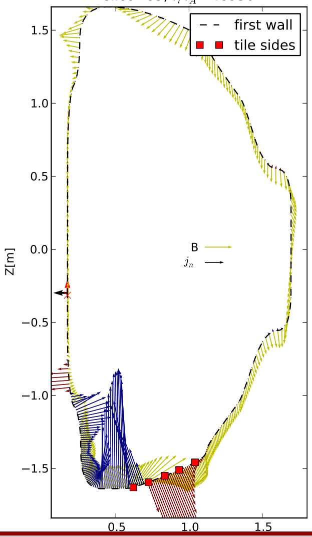

q-profile

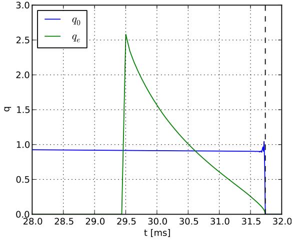

shunt tile currents

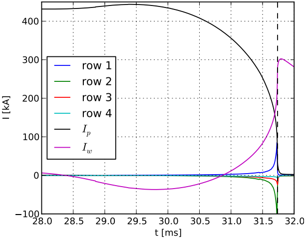

Another M3D-C1 2D nonlinear run of NSTX #132859

with $\eta_W = 5 \times 10^{-4}\Omega m$, $T_h = 24$eV

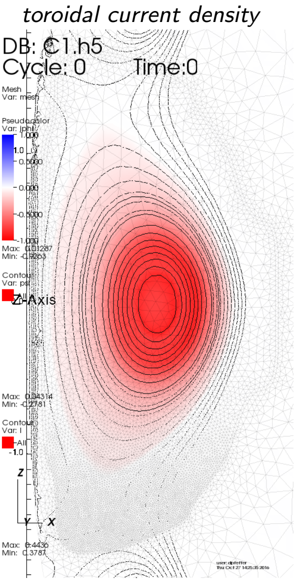

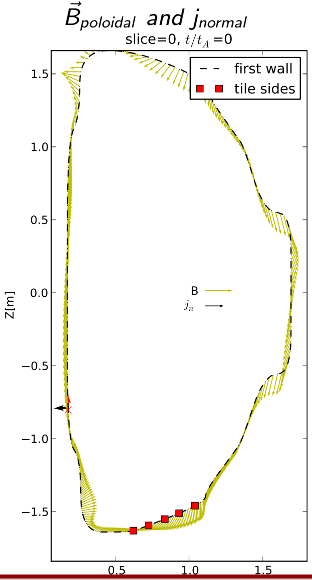

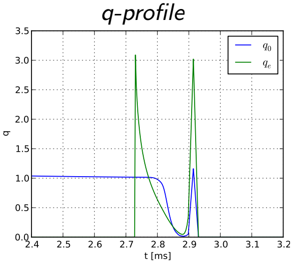

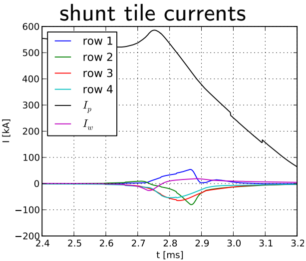

Another M3D-C1 2D nonlinear run of NSTX #132859

with $\eta_W = 5 \times 10^{-4}\Omega m$, $T_h = 24$**eV**

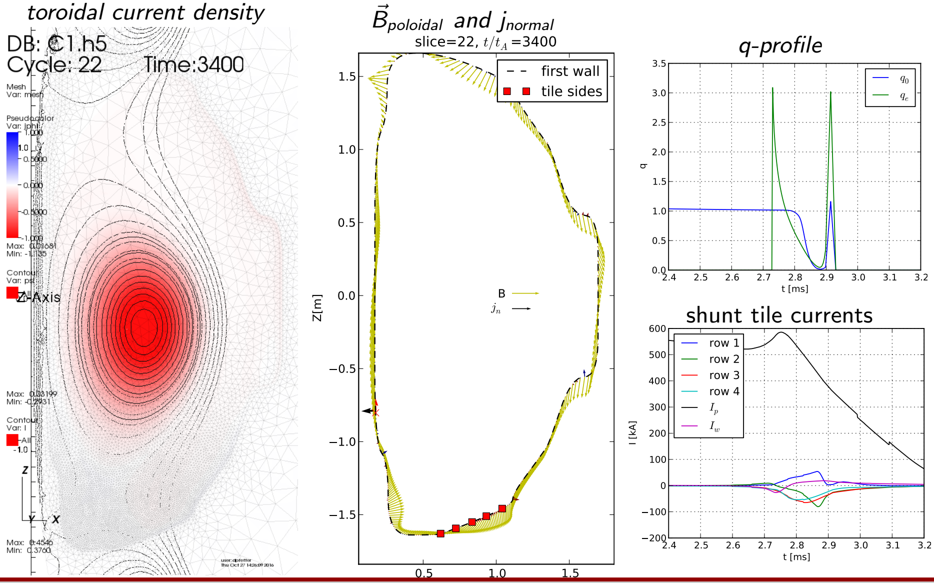

Another M3D-C1 2D nonlinear run of NSTX #132859

with $\eta_W = 5 \times 10^{-4}\Omega m,\ T_h = 24\text{eV}$

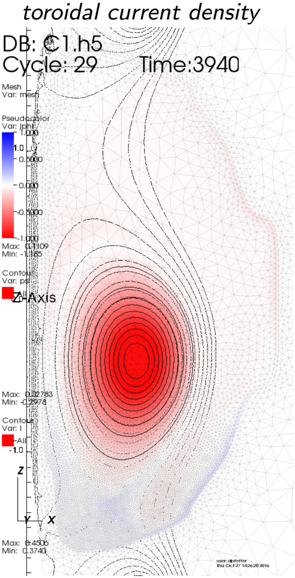

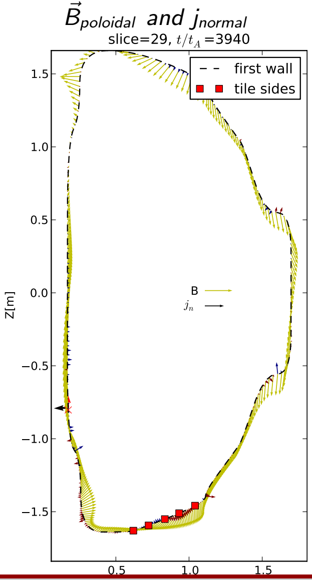

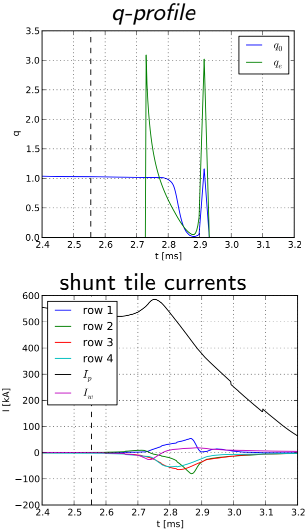

Another M3D-C1 2D nonlinear run of NSTX #132859

with $\eta_W = 5 \times 10^{-4}\Omega m$, $T_h = 24\text{eV}$

toroidal current density

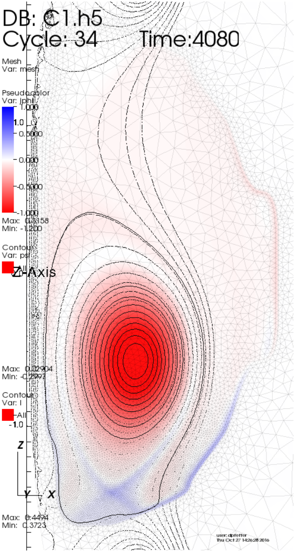

$\vec{B}_{poloidal}$ and j_{normal}

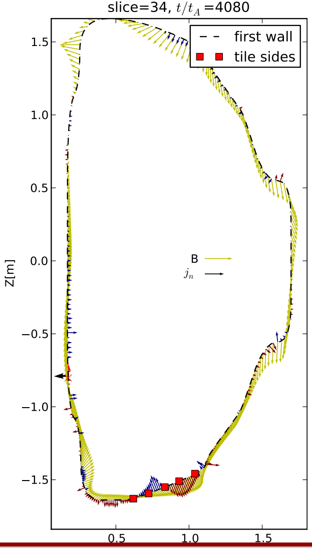

q-profile

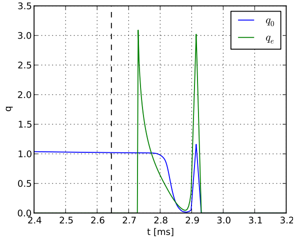

shunt tile currents

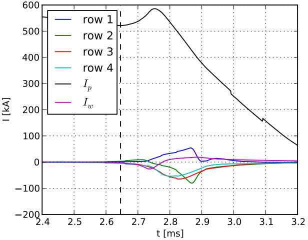

Another M3D-C1 2D nonlinear run of NSTX #132859

with $\eta_W = 5 \times 10^{-4}\Omega m$, $T_h = 24$eV

toroidal current density

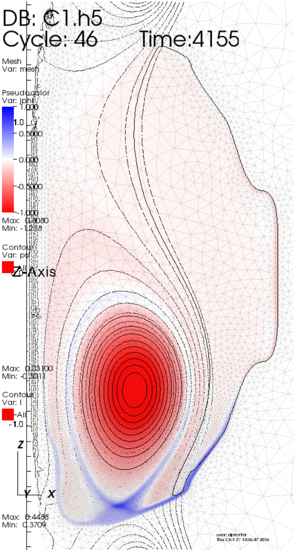

$\vec{B}_{poloidal}$ *and* j_{normal}

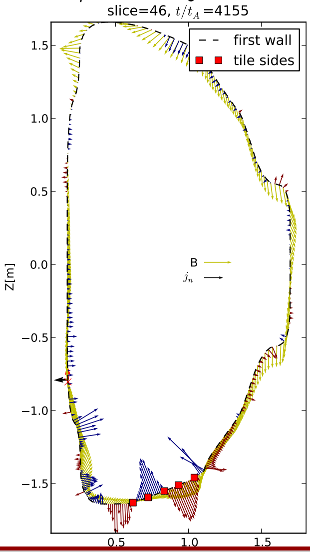

q-profile

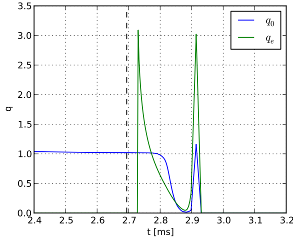

shunt tile currents

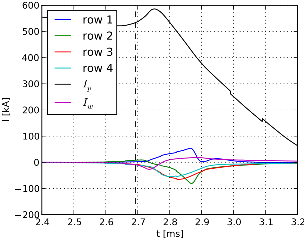

Another M3D-C1 2D nonlinear run of NSTX #132859

with $\eta_W = 5 \times 10^{-4}\Omega m$, $T_h = 24$eV

toroidal current density

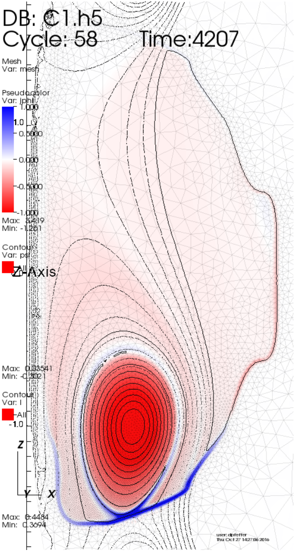

$\vec{B}_{poloidal}$ and j_{normal}

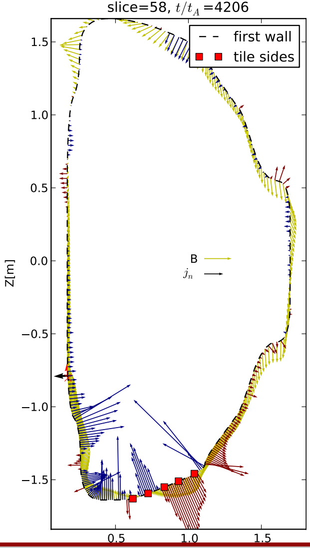

q-profile

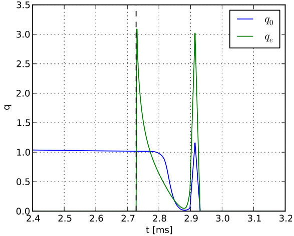

shunt tile currents

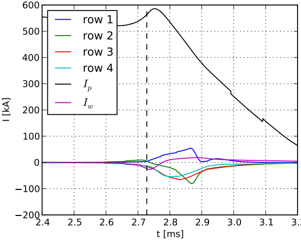

Another M3D-C1 2D nonlinear run of NSTX #132859

with $\eta_W = 5 \times 10^{-4}\Omega m, \; T_h = 24\text{eV}$

toroidal current density

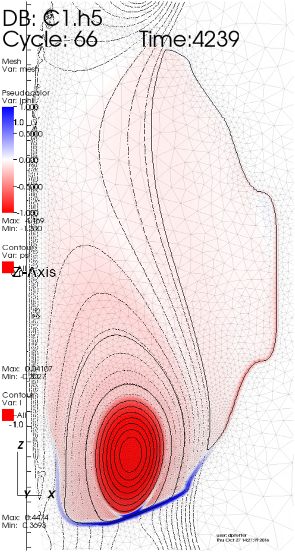

$\vec{B}_{poloidal}$ *and* j_{normal}

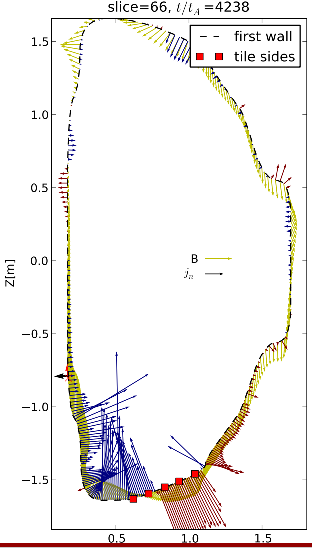

q-profile

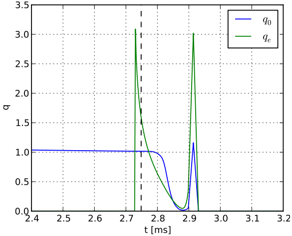

shunt tile currents

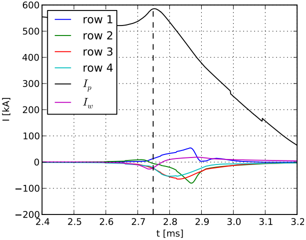

Another M3D-C1 2D nonlinear run of NSTX #132859

with $\eta_W = 5 \times 10^{-4}\Omega m$, $T_h = 24$eV

toroidal current density

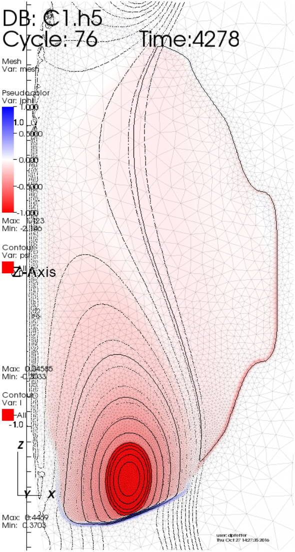

$\vec{B}_{poloidal}$ *and* j_{normal}

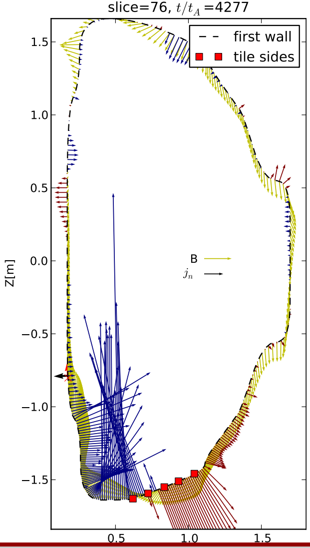

q-profile

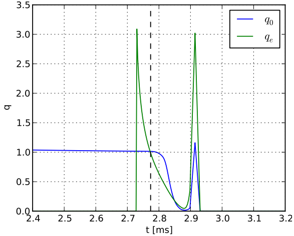

shunt tile currents

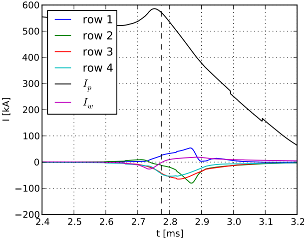

Another M3D-C1 2D nonlinear run of NSTX #132859

with $\eta_W = 5 \times 10^{-4}\Omega m, \; T_h = 24\text{eV}$

toroidal current density

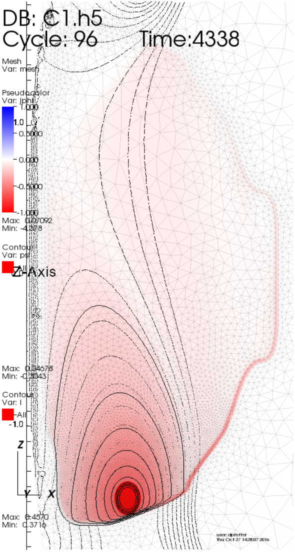

$\vec{B}_{poloidal}$ *and* j_{normal}

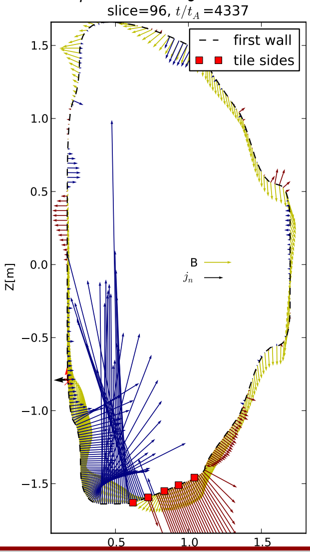

q-profile

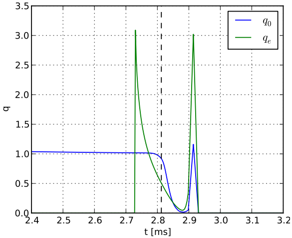

shunt tile currents

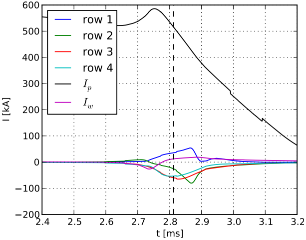

Another M3D-C1 2D nonlinear run of NSTX #132859

with $\eta_W = 5 \times 10^{-4}\Omega m$, $T_h = 24$eV

toroidal current density

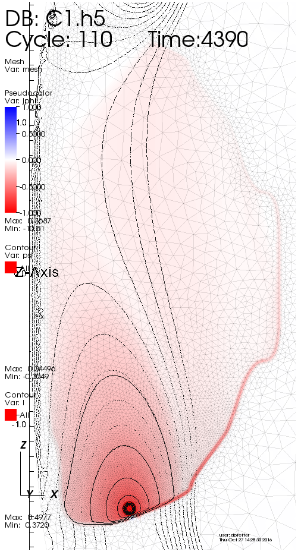

$\vec{B}_{poloidal}$ and j_{normal}

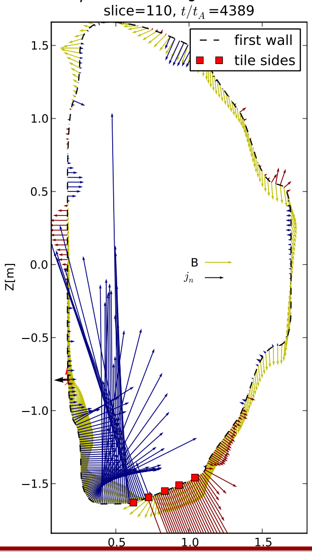

q-profile

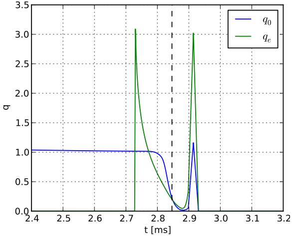

shunt tile currents

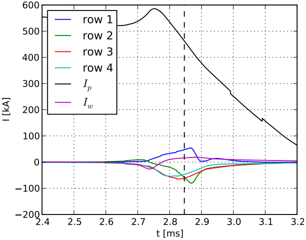

Another M3D-C1 2D nonlinear run of NSTX #132859

with $\eta_W = 5 \times 10^{-4}\Omega m$, $T_h = 24$eV

toroidal current density

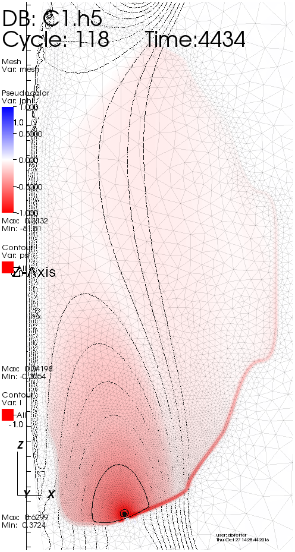

$\vec{B}_{poloidal}$ *and* j_{normal}

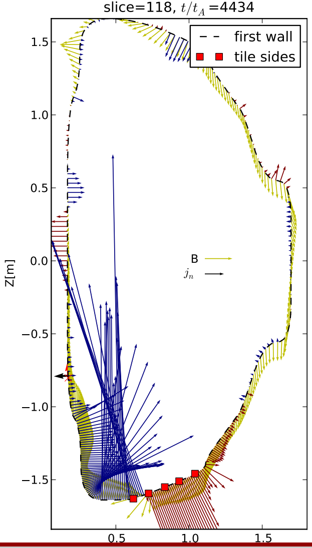

q-profile

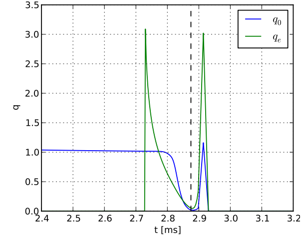

shunt tile currents

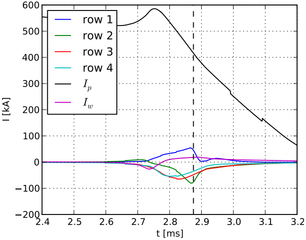

Another M3D-C1 2D nonlinear run of NSTX #132859

with $\eta_W = 5 \times 10^{-4}\Omega m$, $T_h = 24$eV

toroidal current density

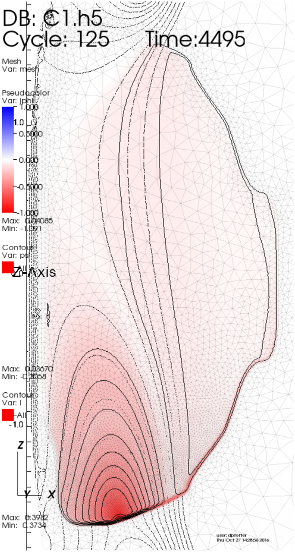

$\vec{B}_{poloidal}$ and j_{normal}

slice=125, t/t_A=4495

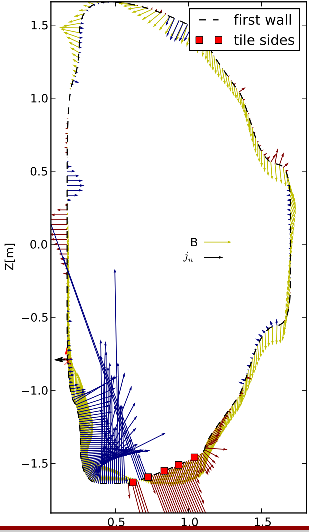

q-profile

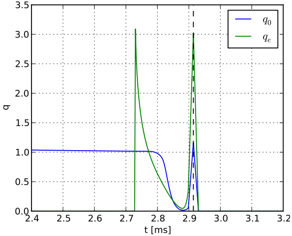

shunt tile currents

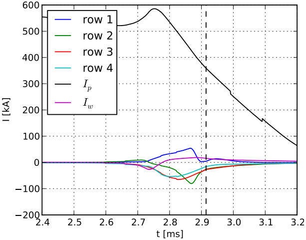

Another M3D-C1 2D nonlinear run of NSTX #132859

with $\eta_W = 5 \times 10^{-4}\Omega m$, $T_h = 24$eV

toroidal current density

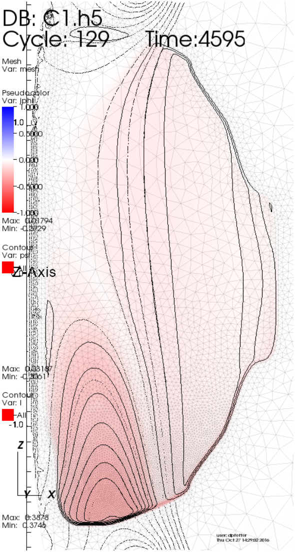

$\vec{B}_{poloidal}$ and j_{normal}

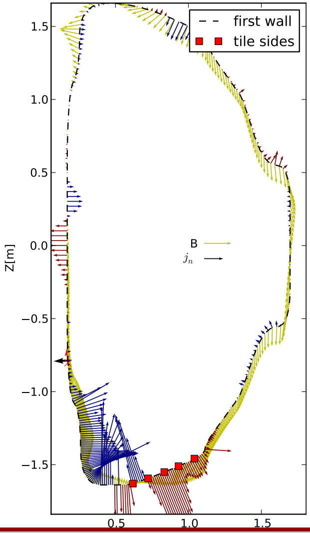

q-profile

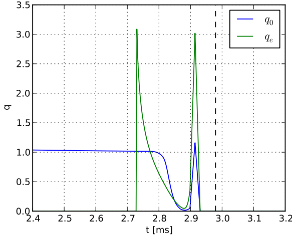

shunt tile currents

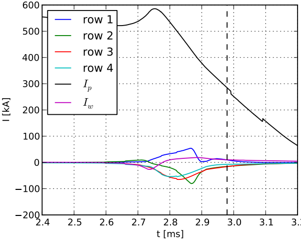

Another M3D-C1 2D nonlinear run of NSTX #132859

with $\eta_W = 5 \times 10^{-4}\Omega m$, $T_h = 24$**eV**

toroidal current density

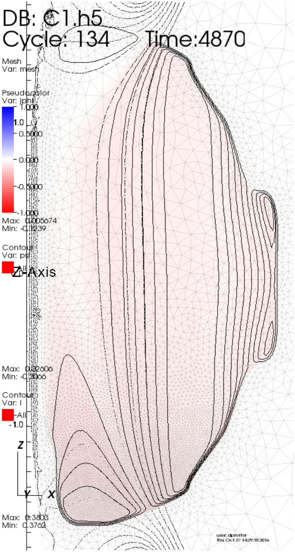

$\vec{B}_{poloidal}$ and j_{normal}

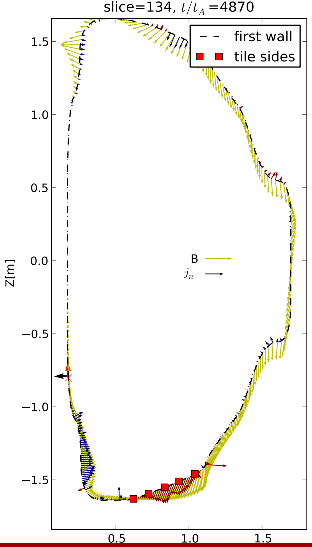

q-profile

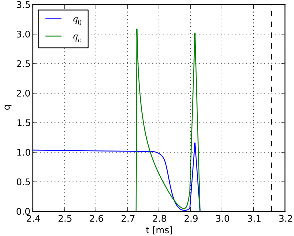

shunt tile currents

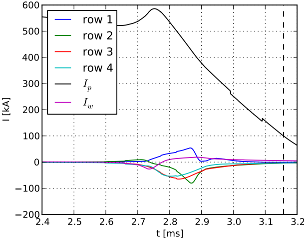

Comments about 2D nonlinear runs

- plasma current is slowly decaying (L_p/R_p) without loop voltage
- current density naturally peaks during slow drift phase $\Rightarrow q_0 < 1$
  - core stability, internal/external inductance (coupling with wall)
  - internal kink can precipitate thermal quench
- $T_h = 9$eV for halo resistivity **reduces induced halo currents**
  - no negative toroidal currents at separatrix
  - plasma current evolution $I_p(t)$ is rounder during quench
    - contact point is narrower $\Rightarrow$ slower flux release
    - later appearance and shorter duration of normal wall currents
  - growth rates decrease with halo temperature (in particular $n = 0$)

Linear analysis informs on non-axisymmetric modes and when to initiate 3D run

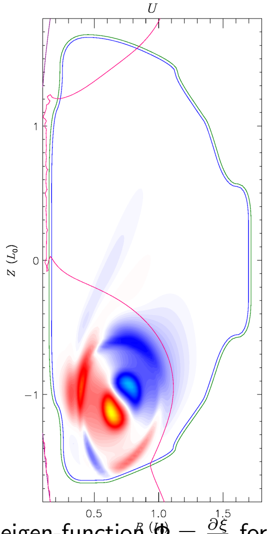

eigen-function $\Phi = \frac{\partial \xi}{\partial t}$ for

$n = 1$ at $t = 45300\tau_A$

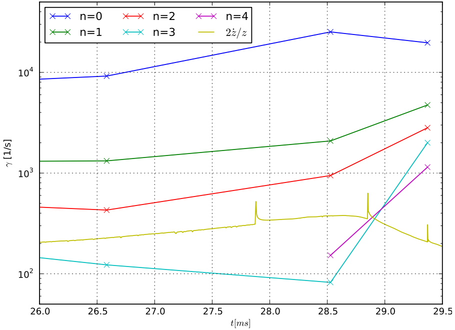

- core modes during drift phase
  - current density peaks causing drop of $q_0 < 1$
  - sawtooth instability could be used as a proxy for thermal quench
- $n = 0$ linear growth-rate from kinetic energy is higher than non-linear evolution of z_{axis}
  - poloidal rotation (sliding) + contraction

3D nonlinear runs launched as plasma contacts wall

Here showing case with $\eta_W = 5 \times 10^{-4}\Omega m$, $T_h = 24$eV

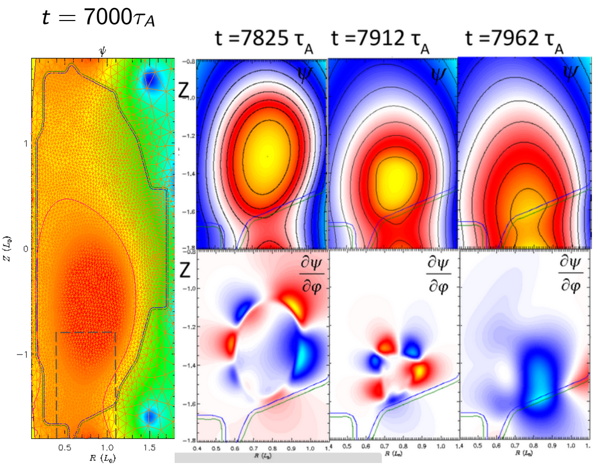

- computationally expensive and sensitive to run
  - 300'000 CPU hours
  - alleviate numerical build-up of gradients via
    - time-step, viscosity, conductivity, resistivity
  - **anisotropic** mesh helps
- non-axisymmetric modes confined to edge
  - halo high temperature, i.e. low resistivity
  - stabilising surface currents
  - stable core to $n > 0$
  - q_e drops below $q_0 \sim 1$

3D nonlinear runs reveal stiff dynamics

Here showing case with $\eta_W = 5 \times 10^{-4}\Omega m$, $T_h = 24$eV

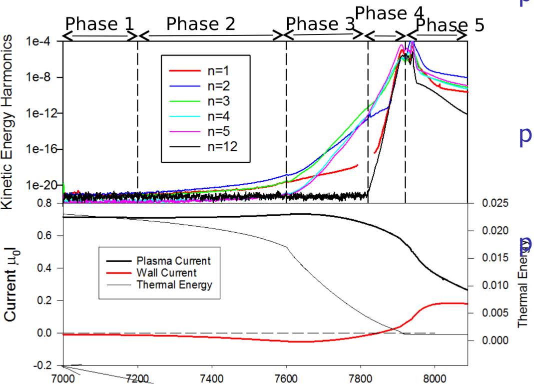

- p.1 drifting plasma (in 3D)
- p.2 vertical motion stalls due to induced $n = 0$ wall currents
  - scrapping-off of LCFS but $q_e > 2$ stable
- p.3 edge surface currents develop as $q_e < 2$
  - stabilise external kink
- p.4 rapid growth of all modes
  - violent termination of plasma as $q_e < 1$
  - complete loss of temperature (flux-surfaces)
- p.5 current decay in residual cold plasma

Virtual diagnostic of 3D normal wall current to compare with shunt tile measurements

normal currents on wall (total)

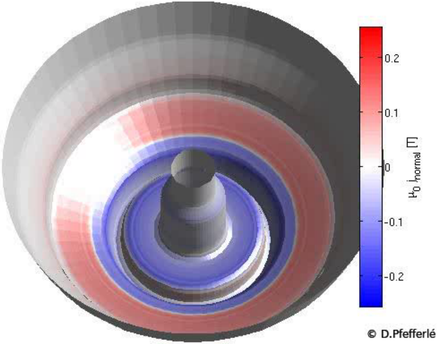

normal currents on wall (non-axisymmetric)

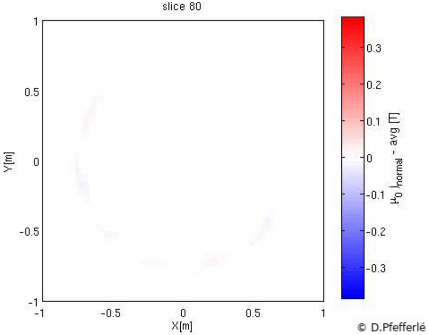

- amplitude quantitatively matches experimental shunt tile
- pattern rotation / zonal component
  - $n = 3 \rightarrow n = 1$, stretching $\rightarrow$ shrinking of current tubes
  - globally zero momentum

1

[1] `C1WC`: post-processing MPI parallelised `FORTRAN` code coupled to `FIO`

Summary and conclusions

- M3D-C1 is employed to model NSTX VDEs with realistic parameters
  - resistive wall capability with finite thickness
  - anisotropic mesh to resolve sharp gradients at plasma/wall contact point
  - implicit scheme to resolve advection-diffusion stiff problem
- faster 2D nonlinear runs are used to meet experimental timescales
- linear analysis to assess growth and structure of non-axisymmetric modes
- massive 3D nonlinear runs for evolution/saturation of non-axisymmetric wall currents
- virtual diagnostics of normal wall currents to compare with experimental data

Ongoing work and future plans

- Simulations, numerics
  - more 2D runs: fine-tuning of wall resistivity, halo temperature, heat conductivity, loop voltage,...
  - as many 3D runs as possible: convergence with toroidal planes, timing of 2D to 3D switching, smoothing/damping of numerical instabilities,...
- Analysis, interpretation and comparison with experimental data
  - sequence of events (z_{mag}, total currents, q-profile) + linear study
  - halo currents, wall forces, mode rotation, torque, TPF,...
  - virtual diagnostics for shunt tiles + magnetic probes
- Extensions and additional effects
  - CHI gap (enforce zero poloidal wall currents)
  - non-uniform / non-axisymmetric wall resistivity
  - toroidal rotation, torque, plasma/wall boundary conditions, sheath physics

Bibliography I

D. Pfefferlé, PPPL (2016).

X. Wesley, Journal (2006).

C. Myers, PPPL (2016).